

Dielectric critical slowing down in ferroelectric $(\text{C}_3\text{N}_2\text{H}_5)_5\text{Sb}_2\text{Br}_{11}$

This article has been downloaded from IOPscience. Please scroll down to see the full text article.

2007 J. Phys.: Condens. Matter 19 406225

(<http://iopscience.iop.org/0953-8984/19/40/406225>)

View [the table of contents for this issue](#), or go to the [journal homepage](#) for more

Download details:

IP Address: 129.252.86.83

The article was downloaded on 29/05/2010 at 06:10

Please note that [terms and conditions apply](#).

Dielectric critical slowing down in ferroelectric (C₃N₂H₅)₅Sb₂Br₁₁

A Piecha and R Jakubas¹

Faculty of Chemistry, University of Wrocław, Joliot-Curie 14, 50-383 Wrocław, Poland

E-mail: rj@wchuwr.chem.uni.wroc.pl

Received 22 June 2007, in final form 16 August 2007

Published 21 September 2007

Online at stacks.iop.org/JPhysCM/19/406225

Abstract

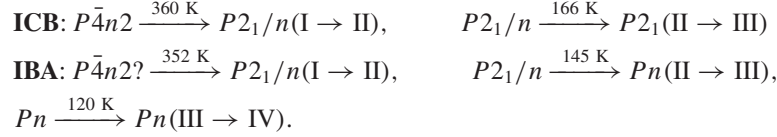
Dielectric dispersion studies have been carried out on the pentakis(imidazolium) undecabromodiantimonate(III), (C₃N₂H₅)₅Sb₂Br₁₁, single crystal in the audio-frequency region. It is found that low-frequency dielectric dispersion, observed for the field along the *a*-axis of the monoclinic symmetry (*P*2₁/*n*), reveals a polydispersive nature near the paraelectric–ferroelectric phase transition temperature (*T*_c = 145 K). The dielectric dispersion results can be fitted with the Cole–Cole formula. Unexpectedly, the mean relaxation frequency obeys the Vogel–Fulcher law with freezing temperature of 143 K. Near the ferroelectric phase transition temperature, the process of dielectric critical slowing down was observed. Such a dynamic dielectric response is characteristic of ferroelectrics with an ‘order–disorder’ transition mechanism.

1. Introduction

Molecular-ionic salts with the general formula R_{*a*}M_{*b*}X_(3*b*+*a*) (R: organic cations, M: trivalent metal ion—Sb or Bi, X: halogen) were extensively studied during the last twenty years. Twelve compounds belonging to this family have been synthesized and studied so far which appear to have ferroelectric properties. The interest has been focused on a mechanism of the ferroelectric–paraelectric transition in these compounds [1–4]. It is shown that ferroelectricity appears in the case of compounds characterized by two-dimensional anionic layers (M₂X₉³⁻) [5–7]. On the other hand, four ferroelectric salts are found to crystallize in the R₅M₂X₁₁ chemical composition, for which the anionic sublattice consists of discrete bioctahedral units Bi₂X₁₁⁵⁻. It is interesting that this type of anionic species is encountered quite rarely and all salts crystallizing with R₅M₂X₁₁ composition, reported to date, appear to have ferroelectric properties [8–11]. Since the dielectric features of the methylammonium analogs: (CH₃NH₃)₅Bi₂X₁₁ (X = Cl, Br) are comparable to those found in well-known TGS-type ferroelectrics, these materials still evoke much interest. Recently, we reported on the

¹ Author to whom any correspondence should be addressed.

ferroelectric properties of two compounds comprising in the crystal structure the imidazolium cations: $(\text{C}_3\text{N}_2\text{H}_5)_5\text{Bi}_2\text{Cl}_{11}$ (abbreviation ICB) [12] and $(\text{C}_3\text{N}_2\text{H}_5)_5\text{Sb}_2\text{Br}_{11}$ (IBA) [13]. Both crystals appear to be isomorphous in the room temperature phase crystallizing in the monoclinic space group, $P2_1/n$. In spite of the fact that they are isomorphous in the paraelectric phase the sequence of the phase transitions was found to be different:



The low-temperature phase (III) of IBA reveals ferroelectric properties with the spontaneous polarization of the order of $1.8 \times 10^{-3} \text{ C m}^{-2}$ along the a -axis. Further cooling of IBA leads to another polar phase (IV) below 120 K, which is also characterized by the reversible spontaneous polarization. The transition mechanism at 166 K in ICB and 145 K in IBA was postulated to be governed by the dynamics of the imidazolium cations [13, 14]. In this paper, we report the dynamic dielectric properties of the $(\text{C}_3\text{N}_2\text{H}_5)_5\text{Sb}_2\text{Br}_{11}$ single crystal in the vicinity of the paraelectric–ferroelectric phase transition temperature ($T_c = 145 \text{ K}$).

2. Experimental details

$(\text{C}_3\text{N}_2\text{H}_5)_5\text{Sb}_2\text{Br}_{11}$ was obtained from an aqueous solution of a stoichiometric mixture of imidazole amine and antimony (III) tribromide with an excess of HBr acid. The single crystals of this compound were grown by a slow evaporation method at constant room temperature (25 °C). The complex dielectric constant, $\epsilon^* = \epsilon' - i\epsilon''$, was measured with an HP 4284A Precision LCR Meter between 100 Hz and 1 MHz. The ac amplitude was 1 V. The samples for dielectric measurements were prepared by cutting the single crystal perpendicularly to the a -axis. The specimen with graphite electrodes had dimensions of $4 \times 4 \times 1 \text{ mm}^3$. The error in the real and imaginary part of the complex dielectric constants was less than 5%.

3. Results and discussion

Plots of the real part of the a -axis relative permittivity ϵ'_a versus temperature at twenty frequencies over the paraelectric phase are displayed in figure 1(a).

Dielectric losses, ϵ''_a , near the phase transition are displayed in figure 1(b). It is clearly seen that the dielectric dispersion becomes remarkable over the frequency range 130 Hz–100 kHz.

The data in figures 1(a) and (b) were subsequently re-plotted as ϵ''_a versus ϵ'_a (Cole–Cole plots) as presented in figure 2. The experimental values of the complex dielectric permittivity $\epsilon^*(\omega)$ can be fit accurately with the phenomenological Cole–Cole formula:

$$\epsilon^* = \epsilon_\infty + \frac{\epsilon_0 - \epsilon_\infty}{1 + (i\omega\tau)^{1-\alpha}} \quad (1)$$

where ϵ_0 and ϵ_∞ are the low- and high-frequency limits of the dielectric constant, respectively, ω is angular frequency, τ is the characteristic relaxation time and α is the parameter, which represents a measure of distribution of the relaxation times.

The fit parameters of the relaxation process are listed in table 1. The Cole–Cole plots (see figure 2) deviate from semi-circles over the temperature region: $T - T_c < 1.2 \text{ K}$. The α parameter ranges from 0.1 up to 0.23 approaching T_c in the paraelectric phase. It indicates that a polydispersive relaxation process in the title crystal takes place. Macroscopic relaxation time (τ) as a function of temperature close to the paraelectric–ferroelectric transition is shown in

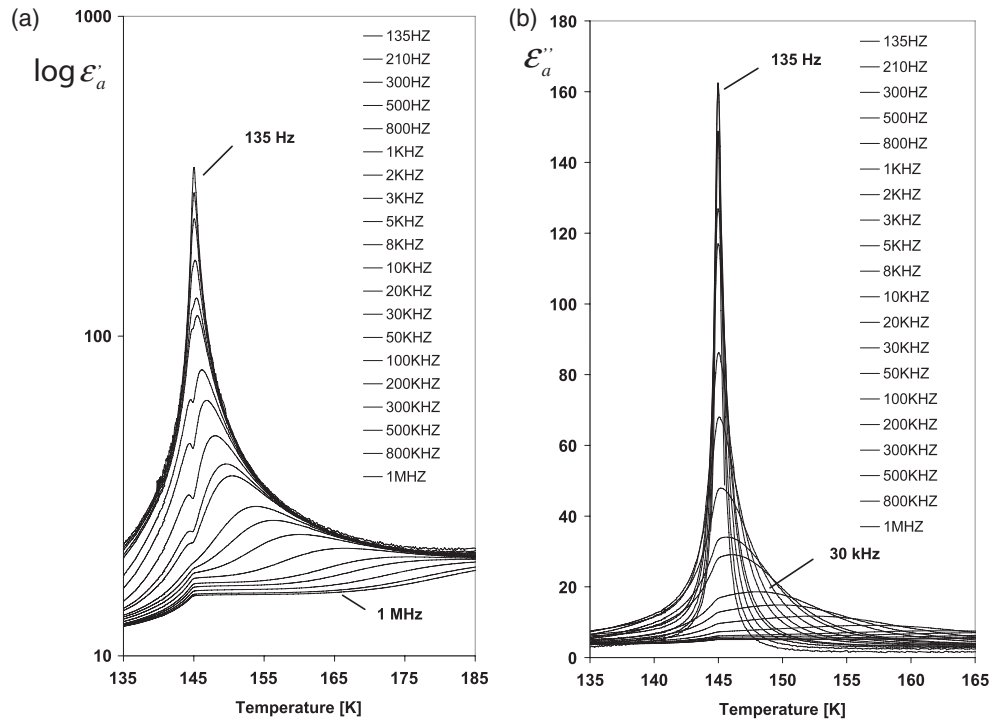


Figure 1. (a) Temperature dependence of the real part ϵ'_a of the dielectric constant at selected frequencies along the a -axis near $T_c = 145$ K in the paraelectric phase (II) (b) Temperature dependence of the imaginary part of the permittivity, ϵ''_a , at selected frequencies in phase (II).

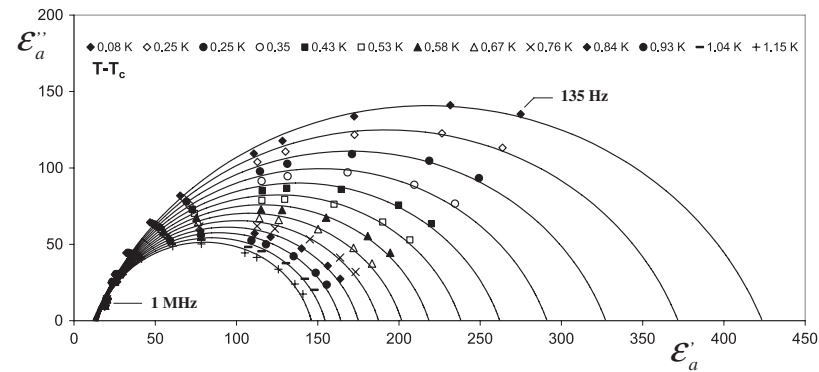


Figure 2. Cole–Cole plots of ϵ''_a versus ϵ'_a at selected temperatures showing the relaxation nature of the dielectric dispersion in the paraelectric phase.

figure 3. The relaxation process in $(C_3N_2H_5)_5Sb_2Br_{11}$ is characterized by an apparent critical slowing down approaching T_c .

The macroscopic relaxation time fulfils the Curie–Weiss law in the paraelectric phase, $\tau \propto (T - T_c)^{-1}$ (figure 3), in a limited temperature region for $\Delta T = T - T_c$ between 0.5 and 3 K. Below 145 K and above 148 K there is observed a clear deviation from a linear part of this relation. It should be emphasized that a presence of critical slowing down of the macroscopic

Table 1. Fit parameters of the relaxation process in $(C_3N_2H_5)_5Sb_2Br_{11}$.

T (K)	ϵ_0	ϵ_∞	α	τ (10^5 s)
145.087	423.57	11.68	0.23	46.7
145.15	371.76	12.17	0.22	37.7
145.25	327.27	12.53	0.21	30.7
145.35	291.09	12.87	0.20	25.4
145.43	262.04	13.11	0.20	21.6
145.53	238.13	13.36	0.19	18.5
145.58	218.47	13.57	0.18	16.2
145.67	201.65	13.81	0.18	14.3
145.76	187.42	13.99	0.17	12.7
145.84	175.00	14.15	0.17	11.4
145.93	164.23	14.31	0.16	10.3
146.04	154.53	14.51	0.16	9.37
146.15	146.09	14.65	0.15	8.57
146.31	131.62	14.91	0.14	7.25
146.72	109.65	15.36	0.13	5.39
146.93	101.28	15.55	0.12	4.73
147.25	90.67	15.80	0.11	3.92
147.48	84.88	15.94	0.10	3.50
148.07	73.19	16.13	0.097	2.68
148.66	64.53	16.27	0.087	2.12
149.16	58.90	16.34	0.080	1.78

relaxation time in a close vicinity to T_c allows us to classify the title compound as a ferroelectric of an ‘order–disorder’ type. The value of τ_0 , characterizing the microscopic relaxator, is related to the macroscopic relaxation time, τ , according to the formula [16]:

$$\tau_0 = \frac{\tau \epsilon_\infty}{(\epsilon_0 - \epsilon_\infty)}. \quad (2)$$

The activation free energy ΔE^* is calculated according to the Eyring equation:

$$\tau_0 = \frac{h}{kT} \exp \frac{\Delta E^*}{kT}. \quad (3)$$

The activation energy ΔE^* is not constant over the analysed temperature range. For the temperatures $T > T_c + 0.5$ K (for ΔT ca 1 K) average ΔE^* was estimated to be 0.39 eV, whereas in the close vicinity of T_c (for $\Delta T = 0.5$ K above T_c) it increases significantly up to 0.78 eV. The observed increase in magnitude of ΔE^* approaching T_c is frequently encountered in the ferroelectric materials. The activation energy for $(C_3N_2H_5)_5Sb_2Br_{11}$ is comparable to that of the $(C_3N_2H_5)_5Bi_2Cl_{11}$ analog (0.47 eV) [12]. The magnitude of ΔE^* is typical of molecular-ionic salts containing bulky organic cations [12, 17]. The relatively large value of ΔE^* may be justified by the fact that the imidazolium cations possessing two heteroatoms of the imidazole ring have a tendency to form a complex network of hydrogen bonds, which additionally stabilize the cations in the lattice.

We decided to fit the dielectric results with the Vogel–Fulcher (VF) equation for two reasons. First, a clear polydispersive relaxation process in the paraelectric phase is observed. Second, non-Eyring behavior of the relaxation time in a wide temperature range was found. It is well-known, that the dielectric properties of the relaxor ferroelectrics (relaxors) and structural glasses [18–20] are described by the phenomenological VF equation [21, 22]. The characteristic feature of these systems is the appearance of a broad temperature and frequency dependent maximum of dielectric permittivity $\epsilon(T, \omega)$ and the extremely slow relaxation below

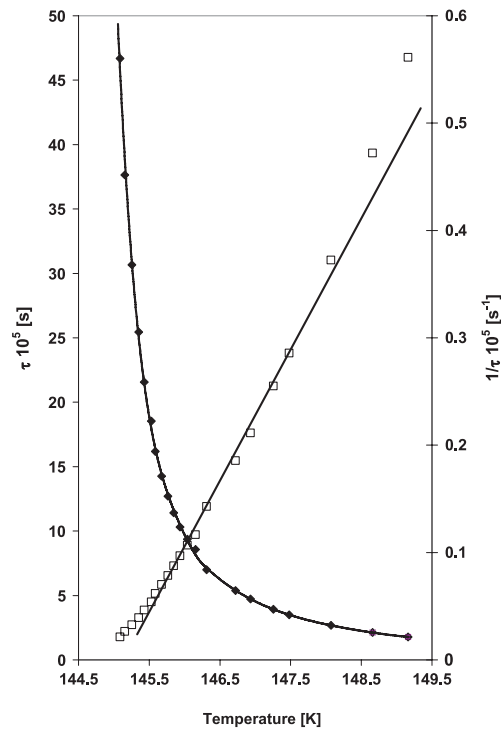


Figure 3. Temperature dependence of the macroscopic relaxation time (τ) and its inverse (τ^{-1}) above T_c (145 K).

T_m (below T_m we have to deal with the onset of relaxor freezing). The mean relaxation frequency follows the Vogel–Fulcher law:

$$\omega = \omega_0 \exp \left[\frac{-E_{aVF}}{k(T - T_{VF})} \right] \quad (4)$$

where: ω_0 —the attempt frequency, E_{aVF} —activation energy for the orientation of electric dipoles, T_{VF} —Vogel–Fulcher temperature (static freezing temperature) and T is the temperature where ϵ'' reaches its maximum value. In the case of $(C_3N_2H_5)_5Sb_2Br_{11}$, the relatively slow relaxation time is especially characteristic of the relaxors, whereas the distribution of the relaxation times is rather moderate. The fitted curves corresponding to the VF equation are presented in figure 4 as a solid line with: $\omega_0 = 2.5 \times 10^5 \text{ s}^{-1}$, $E_{aVF} = 0.096 \text{ eV}$ and $T_{VF} = 143 \text{ K}$. As shown in figure 4, unexpectedly, the VF model describes quite well the relaxation process in the classic ionic ferroelectric— $[C_3N_2H_5]_5[Sb_2Br_{11}]$. The temperature $T_{VF} = 143 \text{ K}$, quite close to the Curie temperature (145 K), is strictly connected with dynamics of the system. The magnitude of E_{aVF} is typical of the ferroelectric relaxors. In our opinion, the dynamics of the imidazolium cations seems to play an important role in the freezing process. It should be noted, however, that one of the VF parameters, namely ω_0 , in our case is relatively low. In various relaxors ω_0 is comparable with the lattice vibration frequencies and ranges from 10^9 to 10^{15} Hz [22].

The crystal structure of both imidazolium analogs: $(C_3N_2H_5)_5Bi_2Cl_{11}$ and $(C_3N_2H_5)_5Sb_2Br_{11}$, is quite complex because in the crystal lattice there are four structurally non-equivalent imidazolium cations present. Three of five cations, being disordered in phase II, are postulated to contribute to the dynamic dielectric permittivity close to T_c . These

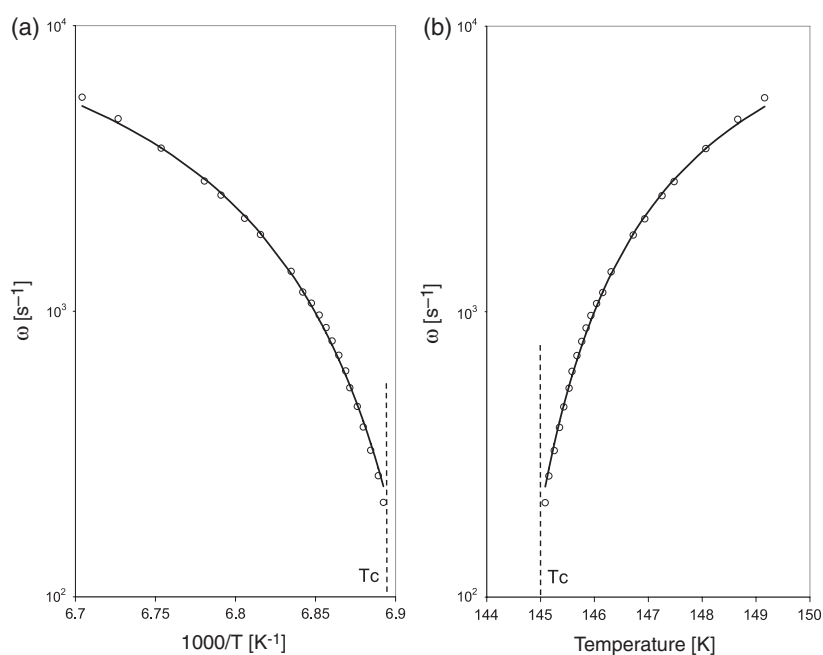


Figure 4. (a) The logarithms of the estimated relaxation frequencies $\omega = 1/\tau$ versus reciprocal temperature $1000/T$ (b) versus temperature. The solid line represents a fit using Vogel–Fulcher relation.

cations are indistinguishable at high temperatures because of significant orientational disorder. Approaching T_c they differentiate themselves. This process is especially marked in $(C_3N_2H_5)_5Bi_2Cl_{11}$, for which the α parameter increases significantly in the close vicinity of T_c , whereas in $(C_3N_2H_5)_5Sb_2Br_{11}$ it is enhanced in a wide temperature range from 0.11 to 0.23 for the temperature interval ca 2.3 K from T_c . On the other hand, it is well-known that the dielectric response in many of the order–disorder ferroelectrics is usually described to a good approximation by the mono-dispersive Debye-type relaxation equation [15]. In our opinion, there may be two reasons for such a dielectric behavior in the bromine analog. First, the dielectric relaxators (imidazolium cations) are better separated in the bromine compound, taking into account their characteristic relaxation times, in comparison to those in the chlorine analog, which may lead apparently to larger distribution of the relaxation process. Second, the single crystals of the bromine analog may be more defected than the chlorine one. The best possibility seems to be related to the fact that $(C_3N_2H_5)_5Sb_2Br_{11}$ is characterized by a very fragile ferroelastic domain structure over the paraelectric phase. The monoclinic angle changes by more than 3° (between 300 and 145 K, [13]) in the bromine analogs, which means that the domain structure continuously rebuilds, influencing the quality of the single crystal sample. On the other hand in the close vicinity of 145 K there a remarkable critical slowing down of the relaxation process is observed with a characteristic minima on the $\epsilon'_a(T)$ curve at T_c . Such a dielectric response is typical of ferroelectric crystals of high quality which are characterized by the order–disorder mechanism of the continuous phase transition [15].

We have succeeded in obtaining, so far, five ferroelectric compounds crystallizing with the chemical stoichiometry $R_5M_2X_{11}$ (where R stands organic cations such as: methylammonium, pyridinium and imidazolium). These ferroelectrics may be divided into two subgroups which are characterized by quite different dynamic dielectric properties and phase transition sequence.

The methylammonium analogs: $(\text{CH}_3\text{NH}_3)_5\text{Bi}_2\text{Cl}_{11}$ and $(\text{CH}_3\text{NH}_3)_5\text{Bi}_2\text{Br}_{11}$, crystallize in the paraelectric phase in the orthorhombic symmetry (Pcab). In the case of methylammonium derivatives, the relaxation process, taking place in the microwave-frequency region, appears to be quite fast [23, 24]. It points out a significant freedom of motion of the methylammonium cations. On the other hand the pyridinium and imidazolium derivatives, were found to crystallize in their paraelectric phases in the monoclinic symmetry ($P2_1/n$). The relaxation process taking place in the audio-frequency region for these salts indicates an important slowing of motion of the aromatic cations near T_c in comparison to that found in the methylammonium salts. One can state, that subtle differences in the structure of these two subgroups are significantly enhanced in their dynamic dielectric properties. The relatively large magnitude of ΔE^* and a long macroscopic relaxation time for salts containing aromatic cations may be explained in terms of various possible hydrogen bond configurations and apparent steric effects. The imidazolium cation possesses two protonodonor sites, thus they are able to form a three-dimensional network of the hydrogen bonds $\text{N-H} \dots \text{Br/Cl}$. The elongation of the relaxation times by nearly 5–6 orders, as compared with those found for the methylammonium analogs [23, 24] in our opinion is a result of fact that the organic moieties are much more strongly stabilized in the crystal lattice than the CH_3NH_3^+ ones.

Static and dynamic dielectric properties of both imidazolium ferroelectrics (ICB, IBA), reveal a significant similarities. The relaxation process taking place within the audio-frequency region is limited to 2–3 K around T_c . The macroscopic relaxation time in both cases reveals a critical slowing down reaching ca 1.1×10^{-3} s for IBA and ca 5×10^{-4} s for ICB close to T_c . It should be emphasized, that the relaxation process in the imidazolium analogs is quite slow as compared to normal ‘order–disorder’ ferroelectrics [15]. We can also distinguish one feature which differentiates these two isomorphous ferroelectrics. The chlorine analog fulfils the Curie–Weiss law (τ versus $(T - T_c)^{-1}$) better than the bromine analog. An extraordinary feature in the case of $[\text{C}_3\text{N}_2\text{H}_5]_5[\text{Sb}_2\text{Br}_{11}]$ is the fact that the dynamic dielectric properties are quite well fitted with the VF equation over the analyzed temperature region. It means that title compound classified as normal ferroelectric exhibits some features characteristic of ferroelectric relaxors or structural glassis.

In conclusion, the dynamic dielectric properties of the imidazolium analogs reflect their structural isomorphism in the paraelectric phase (II). The significant temperature changes of the macroscopic relaxation time both in ICB and IBA compounds clearly show that the phenomenon of the critical slowing down takes place in the imidazolium ferroelectrics and thus confirms the order–disorder mechanism of the paraelectric–ferroelectric phase transitions.

Acknowledgment

This work was supported by the Polish State Committee for Scientific Research (Project Register No. N204 108 31/2551).

References

- [1] Jakubas R and Sobczyk L 1990 *Phase Transit.* **20** 163
- [2] Sobczyk L, Jakubas R and Zaleski J 1997 *Polish J. Chem.* **71** 265 and references cited therein
- [3] Zaleski J and Pietraszko A 1996 *Acta Crystallogr. B* **52** 287
- [4] Bujak M and Angel R J 2005 *J. Solid State Chem.* **178** 2237
- [5] Kallel A and Bats J W 1985 *Acta Crystallogr. C* **41** 1022
- [6] Zaleski J, Pawlaczyk Cz, Jakubas R and Unruh H-G 2000 *J. Phys.: Condens. Matter* **12** 7509
- [7] Jakubas R 1989 *Solid State Commun.* **69** 267
- [8] Lefebvre J, Carpentier P and Jakubas R 1995 *Acta Crystallogr. B* **51** 167

- [9] Matuszewski J, Jakubas R, Sobczyk L and Głowiak T 1990 *Acta Crystallogr. C* **46** 1385
- [10] Jóźków J, Bator G, Jakubas R and Pietraszko A 2001 *J. Chem. Phys.* **114** 7239
- [11] Jakubas R, Piecha A, Pietraszko A and Bator G 2005 *Phys. Rev. B* **72** 104107
- [12] Piecha A, Bator G and Jakubas R 2005 *J. Phys.: Condens. Matter* **17** L411
- [13] Piecha A, Pietraszko A, Jakubas R and Bator G 2007 *J. Chem. Phys.* submitted
- [14] Przesławski J, Kosturek B, Dacko S and Jakubas R 2007 *Solid State Commun.* **142** 713
- [15] Blinc R and Zeks B 1974 *Soft Modes in Ferroelectrics and Antiferroelectrics* (Amsterdam: North-Holland) p 175
- [16] Müser H E and Unruh H-G 1966 *Z. Naturforsch. A* **21** 785
- [17] Baran J, Bator G, Jakubas R and Śledź M 1996 *J. Phys.: Condens. Matter* **8** 10647
- [18] Samara G A 2001 *Solid State Physics* vol 56, ed H Ehrenreich and R Spaepen (New York: Academic)
- [19] Ye Z G 1998 *Key Eng. Mater.* **81** 155
- [20] Samara G A 2003 *J. Phys.: Condens. Matter* **15** R367
- [21] Vogel H 1921 *Phys. Z.* **22** 645
- [22] Fulcher G S 1925 *J. Am. Ceram. Soc.* **8** 339
- [23] Pawlaczyk C, Jakubas R, Planta K, Bruch C and Unruh H-G 1992 *J. Phys.: Condens. Matter* **4** 2695
- [24] Pawlaczyk C, Planta K, Bruch C, Stephen J and Unruh H-G 1992 *J. Phys.: Condens. Matter* **4** 2687